Clinical Cancer Research

Pretreatment microRNA Expression Impacting on Epithelial-to-Mesenchymal Transition Predicts Intrinsic Radiosensitivity in Head and Neck Cancer Cell Lines and Patients

Monique C. de Jong[1,2], Jelle J. ten Hoeve[3], Reidar Grénman[4], Lodewyk F. Wessels[3], Ron Kerkhoven[5], Hein te Riele[1], Michiel W.M. van den Brekel[6,7], Marcel Verheij[1,2], and Adrian C. Begg[1,†]

Abstract

Purpose: Predominant causes of head and neck cancer recurrence after radiotherapy are rapid repopulation, hypoxia, fraction of cancer stem cells, and intrinsic radioresistance. Currently, intrinsic radioresistance can only be assessed by *ex vivo* colony assays. Besides being time-consuming, colony assays do not identify causes of intrinsic resistance. We aimed to identify a biomarker for intrinsic radioresistance to be used before start of treatment and to reveal biologic processes that could be targeted to overcome intrinsic resistance.

Experimental Design: We analyzed both microRNA and mRNA expression in a large panel of head and neck squamous cell carcinoma (HNSCC) cell lines. Expression was measured on both irradiated and unirradiated samples. Results were validated using modified cell lines and a series of patients with laryngeal cancer.

Results: miRs, mRNAs, and gene sets that correlated with resistance could be identified from expression data of unirradiated cells. The presence of epithelial-to-mesenchymal transition (EMT) and low expression of miRs involved in the inhibition of EMT were important radioresistance determinants. This finding was validated in two independent cell line pairs, in which the induction of EMT reduced radiosensitivity. Moreover, low expression of the most important miR (miR-203) was shown to correlate with local disease recurrence after radiotherapy in a series of patients with laryngeal cancer.

Conclusions: These findings indicate that EMT and low expression of EMT-inhibiting miRs, especially miR-203, measured in pretreatment material, causes intrinsic radioresistance of HNSCC, which could enable identification and treatment modification of radioresistant tumors. *Clin Cancer Res; 21(24); 5630–8. ©2015 AACR.*

Introduction

Radioresistance of head and neck cancer

Radiotherapy is the most important treatment modality in head and neck cancer, with two thirds of patients treated with (chemo-)radiotherapy (1). With altered fractionated radiotherapy, the locoregional control rates for earlier stages are encouraging, but for stage III and IV tumors, locoregional control remains around 50% (2), leaving considerable need for improvement. Factors that contribute to control of the tumor are tumor site, stage, treatment schedule and dose, tumor volume, and HPV status (3–5). However, even after correcting for these factors, there are still differences in control rates. Such differences may result from differences in tumor microenvironment, tumor cell properties like hypoxia, rapid repopulation between fractions, the fraction of cancer stem cells or intrinsic radiosensitivity (6).

Intrinsic or cellular radiosensitivity is a term used to describe the process of one tumor cell being more resistant than another on the basis of different intracellular mechanisms, independent of microenvironmental factors.

An appropriate way to study intrinsic radiosensitivity is therefore in tissue culture in which potential confounding factors can be reduced or eliminated. It has indeed been shown that intrinsic cellular radiosensitivity significantly determines the outcome of radiotherapy in head and neck cancer (7). However, these data were attained using functional (cell survival) studies, giving limited or no information on genes or pathways involved and thus providing little help to the treating physician on how to improve treatment for patients with radioresistant tumors. We therefore searched for genetic and thus potentially assessable and

[1]Department of Biological Stress Response, The Netherlands Cancer Institute, Amsterdam, the Netherlands. [2]Department of Radiation Oncology, The Netherlands Cancer Institute, Amsterdam, the Netherlands. [3]Department of Computational Cancer Biology (Department of Molecular Carcinogenesis), The Netherlands Cancer Institute, Amsterdam, the Netherlands. [4]Department of Otorhinolaryngology–Head and Neck Surgery and Department of Medical Biochemistry, Turku University Hospital, University of Turku, Turku, Finland. [5]Central Genomic Facility, The Netherlands Cancer Institute, Amsterdam, the Netherlands. [6]Department of Head and Neck Oncology and Surgery, The Netherlands Cancer Institute, Amsterdam, the Netherlands. [7]Department of Maxillofacial Surgery, Academic Medical Center, University of Amsterdam, Amsterdam, the Netherlands.

Note: Supplementary data for this article are available at Clinical Cancer Research Online (http://clincancerres.aacrjournals.org/).

[†]Deceased.

Corresponding Author: Marcel Verheij, Divisions of Biological Stress Response and Radiation Oncology, The Netherlands Cancer Institute, Plesmanlaan 121, Amsterdam 1066 CX, the Netherlands. Phone: 31-20-5122035; Fax: 31-20-5121792; E-mail: m.verheij@nki.nl

doi: 10.1158/1078-0432.CCR-15-0454

Translational Relevance

In head and neck squamous cell carcinomas (HNSCC), radiation is a major treatment modality. Intrinsic radioresistance of tumor cells is one of the predominant causes of head and neck cancer recurrence. This phenomenon can only be examined by *ex vivo* colony assays, but these take too much time to be clinically useful and do not reveal the biologic mechanisms of intrinsic radioresistance. Using microRNA and mRNA expression profiles of HNSCC cell lines and tumors, we found that low expression of certain microRNAs that suppress epithelial-to-mesenchymal transition, measured prior to treatment, is causally related to intrinsic resistance to radiation. This finding provides an important step toward modification and thereby improvement of the treatment of radioresistant tumors.

targetable factors that affect intrinsic radioresistance in head and neck cancer.

mRNA to study radioresistance

mRNA profiling has been used to study radioresistance in cell lines. To date, however, such experiments have been mostly performed on either one or two cell lines only, or on the NCI-60 cell line panel, which contains no head and neck squamous cell carcinoma (HNSCC) lines (8, 9). Because it is known that radiosensitivity is partly dependent on the tissue of origin (e.g., lymphomas are more sensitive than solid tumors), use of such a cell line panel to predict HNSCC radiosensitivity is of questionable value. Therefore, Hall and colleagues attempted to identify a robust gene signature associated with intrinsic radiosensitivity on a series containing 16 cervical and 11 HNSCC cell lines. Unfortunately, they failed to identify such a set (10). Possibly this could be attributed to the fact that mRNA levels alone give an incomplete picture of active processes in the cell, as other factors can influence translation to protein. Among these are microRNAs (miR).

microRNAs

miRs are genomically encoded small pieces of single-stranded RNA of around 22 nucleotides each of which can silence hundreds of genes (11). More than 1,000 miRs have been identified so far, estimated to regulate expression of at least 60% of all genes (12). miRs regulate gene expression by binding to their (partly) complementary sequence on mRNA molecules, resulting in reduced protein production (13, 14). miRs can reduce protein production by causing degradation of mRNAs or by inhibiting translation. Multiple modes of silencing thus seem to exist that can be active concurrently (15, 16).

Ionizing radiation has been shown to induce significant changes in miR expression in 6 cancer cell lines (17). miRs playing a role in radioresistance have been described, although experiments were done in cell line pairs and not in a larger panel of cell lines (18–20).

Study goal

The goal of this study was therefore to get a better insight into the genetic causes of intrinsic radioresistance in head and neck cancer cells focusing on miR expression. Using a large panel of HNSCC cell lines, we aimed to answer the following questions: (i) Do miR/mRNA expression changes induced by irradiation correlate with radioresistance?; (ii) Can we identify mRNAs that correlate with radioresistance?; (iii) Can we identify driving miRs that correlate with radioresistance?; (iv) If so, are these miRs and their targets related to certain pathways or processes?; and (v) Finally, do these miRs correlate with radiotherapy response in patients with laryngeal cancer? The answers to these questions should lead to a better understanding of radioresistance in this disease and therefore provide guidance toward more individualized treatment.

Materials and Methods

Cell line selection and culture

Cell line selection. All cell lines for hypothesis generation were obtained from Professor R. Grénman (University of Turku, Turku, Finland), who has a unique panel of more than 100 well-characterized HNSCC cell lines with known radiosensitivity. We selected 32 HNSCC cell lines from different subsites (Supplementary Table S1). Cell lines previously treated with chemotherapy or derived from metastatic sites other than regional lymph nodes were excluded.

Cell culture. All cells were cultured in DMEM, supplemented with 1% L-glutamine, 1% nonessential amino acids, 10% FBS, and antibiotics. Cells were incubated in humidified air with 5% CO_2 at 37°C. Depending on the doubling time, cells were subcultured every 3 to 14 days to ensure exponential growth. Cells were used for experiments when they were around 60% to 70% confluent. Preferably, low passages (10–20) were used.

Validation cell lines. The UT-SCC-43A and UT-SCC-43A-Snail cell lines were developed and provided by Dr M. Takkunen (University of Helsinki, Helsinki, Finland; ref. 21). The FaDu-cDNA3 and FADU-HIF1α(ΔODD) cell lines were developed and provided by Prof. Kou-Juey Wu (National Yang-Ming University, Taiwan, ROC; ref. 22). Both cell lines are human HNSCC, transfected with either the transcription factor snail or HIF1α with a deleted oxygen degradation domain, thereby causing the cells to undergo epithelial-to-mesenchymal transition (EMT).

Irradiation assay

Radiosensitivity assay. Radiosensitivity of all cell lines was tested with a 96-well plate clonogenic assay, developed by Grénman and colleagues (23, 24). The radiosensitivity of a cell line was defined as the area under the survival curve, with measurements of the survival fraction at 6 different doses, each repeated at least 3 times. When a comparison was made between radioresistant and radiosensitive cell lines, the cutoff was set at a median area under the curve of 2.0.

RNA collection after irradiation. Cells were irradiated using a ^{137}Cs irradiation unit with a dose rate of 0.662 Gy/min. Mock-irradiated cells were harvested for all cell lines, as well as cells at 2 and 6 hours after 4 Gy. At the given time points, cells were rinsed with ice-cold PBS twice and then collected in RNA-Bee (Campro Scientific).

RNA isolation from cell lines

All steps from RNA isolation to microarray hybridization were performed at the Institute's central microarray facility. Cells in

RNA-Bee were used to extract total RNA. The sample was then split into two for analysis of miR and mRNA separately. mRNAs were further purified using the RNeasy Mini Kit and the RNase-Free DNase Set from Qiagen. The RNA was isolated and DNAse treated using the spin columns according to the manufacturer's instructions. The Agilent 2100 Bioanalyzer was used to confirm the presence of intact RNA.

mRNA/miR microarrays in cell lines

mRNA. Biotin-labeled cRNA was generated using the Illumina TotalPrep RNA Amplification Kit (AMIL1791, Ambion Inc.). Briefly, to synthesize biotin-labeled cRNA, 350 ng of total RNA was reversed transcribed and subsequently amplified and labeled with biotin (*in vitro* transcription). Next, the cRNA (1,500 ng per array) was hybridized to v3 Illumina bead arrays according to the manufacturer's instructions (Illumina, Inc.). Array signals were developed by Amersham fluorolink streptavidin-Cy3 (GE Healthcare Bio-Sciences) following the BeadChip manual. Fluorescence intensities were measured with the scanner and averaged per probe. Background adjustment was done using the method from the affy package, after which data were $\log_2$-transformed and robust spline normalized. As a final step, annotations were updated using the lumiHumanAll package (25) in R and subsequently the data were aggregated per gene symbol: data from probes with the same gene symbol and a correlation greater than 0.7 were averaged.

microRNAs. Using the Exiqon miRCURY LNA microRNA Array kit (fifth generation), 1 μg total RNA was labeled with Hy3 and hybridized in a TECAN HS4800 Hybridization Station against the slides together with a reference pool of all samples (Hy5). The slides were scanned in a DNA Microarray Scanner (Model G250B, Serial number US22502518) from Agilent Technologies, which uses Scan Control software (Version A.6.11). After subtraction of the mean background signal, arrays were $\log_2$-transformed and normalized using the LOWESS method (using Imagene 6.0 software).

Patient series

Patient selection. Thirty-four patients treated at The Netherlands Cancer Institute (Amsterdam, the Netherlands) between 2002 and 2010 were selected as a validation cohort. To avoid confounding by the addition of surgery or chemotherapy, a cohort consisting of patients with T2-3 laryngeal cancers was compiled. These patients were all treated with radiotherapy alone with a curative intent. The series was designed to be a matched cohort of 17 patients with local recurrences matched with 17 local cures. There were no significant differences between groups with and without local recurrence in age, gender, subsite, T-stage, or treatment year (Supplementary Table S2).

miR extraction. Using the Roche High Pure miRNA Isolation Kit (REF: 05080576001), miRNAs were extracted from pretreatment biopsies. Briefly, 5 slides of 5-μm thickness were deparaffinized and macrodissected, assuring that the sample consisted of at least 50% tumor cells. miRs were further purified according to the manufacturer's instructions.

miRNA library preparation and sequencing

The total RNA samples were quality-controlled and quantified with the Agilent Technologies 2100 Bioanalyzer, using the RNA 6000 Nano kit. One microgram of total RNA in a volume of 5 μL was used as input for the miR library preparation for Illumina sequencing (SR 50bp) using the TruSeq Small RNA Sample Preparation Kit (RS-200-0012) and Guide (Part # 15004197 Rev. E). Shortly, stepwise RNA ligation of 3′ and 5′ adapters to miRs introduce a specific index to every sample. The product was PCR-amplified and pooled and purified using a 6% PAGE gel. Fragments of 145 to 160 bp were cut from the gel, washed and concentrated by ethanol precipitation, and resuspended in nuclease-free water. The small RNA library pools were quantified using a DNA 7500 chip with the Agilent Technologies 2100 Bioanalyzer. The pools were diluted to a concentration of 2 nmol/L and passed on for sequencing onto an Illumina HiSeq2000 machine and a stretch of 50 bp was sequenced according to manufacturer's instructions. The FAST-Q data from the run were analyzed and quantified by comparing the data to the miR databases.

Sequence reads (51 bp) were mapped using the mirExpress pipeline. The reads were trimmed for adapter sequences upon alignment. During the alignment, the identity was set to 0.9. Human mature and precursor sequences were downloaded from miRbase (version 20). The miR expression results that were generated for each sample were combined for further analysis. miR counts were normalized to 100,000 reads per patient.

Analysis

Time course analyses were performed using the Biometric Research Branch (BRB) ArrayTools (http://linus.nci.nih.gov/BRB-ArrayTools.html). This is a tool that performs a regression analysis of time course data, finding patterns that correlate with time, class, or both. Pathways and networks were analyzed through the use of Ingenuity Pathway Analysis (IPA; Ingenuity Systems, www.ingenuity.com). Cell survival curves were generated and analyzed in GraphPad Prism 6.0. All other analyses were performed in R (26), using the Bioconductor packages (27) and our own scripts.

miR target selection

Because most miR–mRNA interactions are predicted interactions on the basis of the complementarity of their RNA sequences and not on experimentally validated interactions, a collection of the most likely mRNA targets was generated for each miR by analysis of validated interaction data from external databases. A maximum of 750 mRNA targets per miR were selected on the basis of our own prediction model trained to predict experimentally validated targets from Tarbase 6.0 (28) on miR and target properties from TargetScanHuman 6.2 (14, 29). A list of these interactions is available in supplementary Text File S1.

Results

Data overview

All tested cell lines responded to irradiation by profound changes in gene expression. To investigate whether this response correlates with radioresistance, we determined the abundance of 18,913 unique mRNAs at 0, 2, and 6 hours after 4 Gy and of 279 unique miRs at 0 and 6 hours after 4 Gy in 32 HNSCC cell lines (Fig. 1).

1. MiR/mRNA expression changes 2 and 6 hours after 4 Gy do not correlate with radioresistance. Thousands of mRNAs and miRs showed expression changes in one or more of the cell lines in

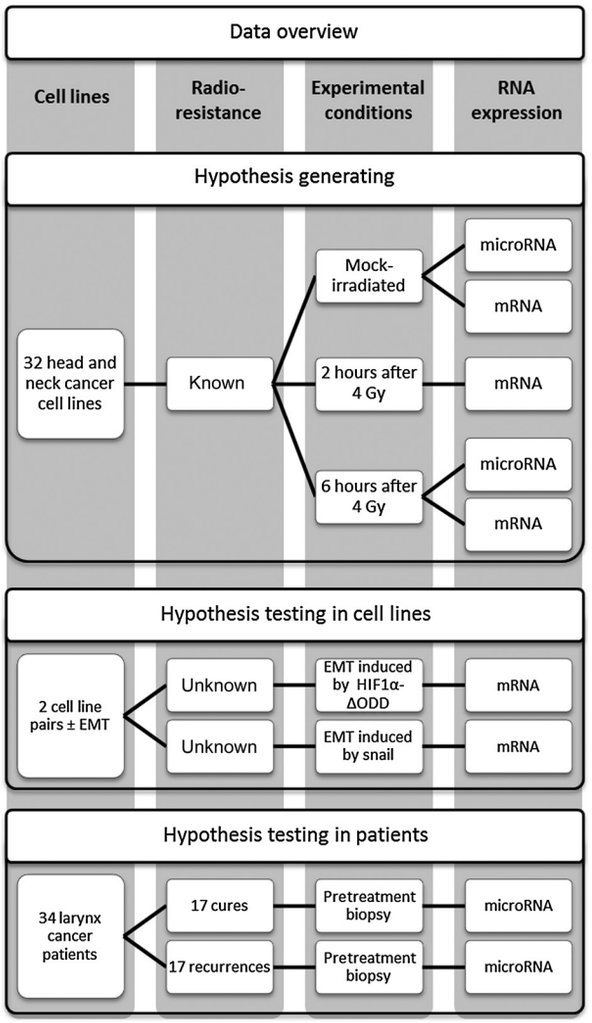

Figure 1.
Overview of data.

response to 4 Gy. The time course plug-in in BRB array tools identifies cell lines with similar gene up- or downregulation after irradiation. An expression response pattern common to all 32 cell lines involved 175 genes (Supplementary Fig. S1), none of them encoding miRs. When analyzing these common response genes in IPA, the most significant canonical pathways were associated with protein ubiquitination, cell-cycle regulation, and DNA double-strand break repair.

When genes with an altered expression 6 hours after 4 Gy (compared with baseline expression) were subjected to cluster analysis, 2 main response clusters became evident. Genes that were different between the 2 response clusters were analyzed in IPA, which showed that 11 cell lines in the first cluster had an activated TP53 and HNF4A response, whereas this response was inhibited in the other 21 cell lines. However, the 2 clusters showed no correlation with radioresistance (*t* test; $P = 0.82$).

The time course plug-in also searches for response patterns that are significantly different between 2 groups. Here we found that changes 2 and 6 hours after 4 Gy did not differ between the 14 radiosensitive and 18 resistant cell lines, neither in mRNA nor in miR expression.

*2. **mRNAs and radioresistance.*** The BRB time course plug-in further analyzes the difference between sensitive and resistant cell lines, independent of the time response. In this analysis, 1,226 genes with a stable expression over the 3 time points significantly correlated with radioresistance using a false discovery rate cutoff of <0.05 (Supplementary Table S4). In addition, separate *t* tests were performed between the expression of the sensitive and resistant groups for each of the 3 time points. The 3 resulting *P* values were then pooled per gene. The expression over time for the top 5 positively and negatively correlated genes (i.e., with the lowest pooled *P* value) is shown in Fig. 2A and B. An IPA showed that these 1,226 genes corresponded mostly with the following molecular and cellular functions: cellular movement, cellular development, cellular growth and proliferation, cell-to-cell signaling, and interaction and cell morphology. These functions are suggestive of a role for EMT, which describes a process in the cell that leads to loss of polarity, increased migratory and invasive capacity, and reduced cell–cell contact (30).

*3. **Identification of miRs that correlate with radioresistance.*** To find driving miRs that influence radioresistance, we set 3 separate requirements: (i) to select miRs that were actively degrading their mRNA targets, there had to be a negative correlation between miR expression and expression of its targets; (ii) a correlation between miR expression and radioresistance; and (iii) an inverse correlation of the target expression with radioresistance (compared with the miR–radioresistance correlation). Using these criteria, the chance of finding false-positive results is brought down to a minimum and only relevant miRs are identified.

For this analysis, miRs and mRNAs were filtered on the basis of the interquartile range (IQR) of expression between the 32 cell lines to exclude uninformative values. This left 200 miRs and 13,041 mRNAs with an IQR higher than 0.5 for the analysis. Of the 200 miRs, 39 were discarded because they had fewer than 5 predicted targets. After the filtering steps, the remaining 161 miRs had an average number of 506 predicted mRNA targets, as defined by our *in silico* generated miR–mRNA interaction database. Of these 161 miRs, 37 had a significantly negative miR target Pearson correlation after multiple testing correction. *P* values for the correlation between each miR and its targets were calculated using a two-sided *t* test of the Pearson correlations of the predicted mRNA targets for each miR versus the Pearson correlations of all other (random) mRNAs with the miR expression. *P* values for the correlation between mRNA targets and radioresistance were calculated using the same approach, comparing the difference between all *P* values for the Pearson correlations between the targets and radioresistance versus all *P* values for the correlations between the nontarget mRNAs and radioresistance. *P* values for the difference in miR expression between sensitive and resistant cell lines over the two time points were obtained using the BRB time course plug-in. A significant correlation of the miR and its targets with radioresistance was observed for 12 of these 37 miRs, belonging to 10 different miR families (Table 1). Expression over time for the top 5 miR families can be seen in Fig. 2C. Of interest is that 292 of the earlier identified 1,226 mRNAs that were significantly correlated with radioresistance are being regulated by one of these 12 miRs.

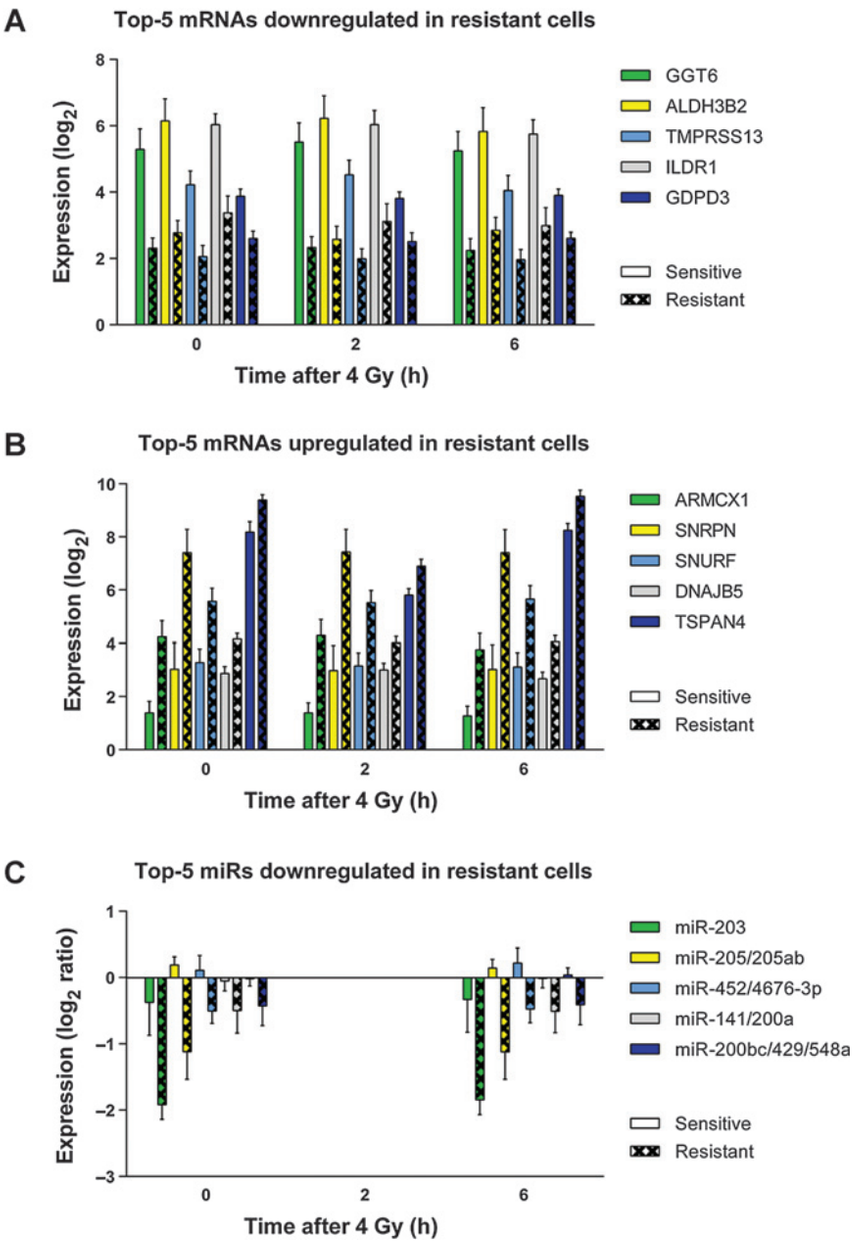

Figure 2.
MiR and mRNA expression differences between resistant and sensitive cell lines. mRNA and miR expression differences between sensitive and resistant cell lines over time. The differences between sensitive and resistant cell lines at the individual time points were all individually significant (*t* test; $P < 0.05$), except for miR-141/200a and miR-200bc/429. The differences between sensitive and resistant cells for these two miR families were only significant, when the measurements at both time points were considered. Error bars, mean ± SEM.

4. EMT correlates with radioresistance. From the data described in mRNAs and radioresistance and Identification of miRs that correlate with radioresistance, it appears that the loss of miRs downregulating EMT mRNAs were significantly correlated with the intrinsic radioresistance of these 32 HNSCC cell lines.

To verify that EMT had a causal relation with radioresistance, we collected 2 HNSCC cell lines that had been forced to undergo EMT: UT-SCC-43A-Snail and FaDu-HIF1α(ΔODD). Both Snail and HIF1α are known transcription factors for EMT. In cell culture, the Snail- or HIF1α-expressing cells were clearly mesenchymal, whereas the respective control cells lines UT-SCC-43A and FaDu-cDNA3 had an epithelial growth pattern. In these pairs, we found that the cells that had undergone EMT were significantly more resistant to radiotherapy (Fig. 3), with areas under the survival curve increasing from 2.7 to 3.9 ($P < 0.0001$) in the FaDu pair and from 2.6 to 4.6 ($P < 0.0001$) in the UT-SCC-43A pair.

We further tested the correlation between radiosensitivity and processes known to influence radiotherapy response in the 32 cell lines, by using published gene sets for reactive oxygen species (31), hypoxia (32, 33), proliferation (34), stem cells (single marker CD44 and the set from ref. 35), p53 (constructed ourselves, Supplementary Table S5), DNA repair (constructed ourselves, Supplementary Table S5), and intrinsic radiosensitivity (8, 9). We also constructed our own HNSCC EMT signature from the two pairs of HNSCC cell lines in which EMT was induced. This signature was constructed from genes with a fold change greater than 2 or under 0.5 between parental and EMT-induced strains. In

Table 1. Relevant miRs correlated with radioresistance

miRs correlated with radioresistance						
				5. Correlation with radioresistance		
1. miR name	2. Predicted mRNA targets, *n*	3. Significant negative miR–mRNA targets correlation? (*P*)	4. miR expression in resistant cells up or down?	a. miR only (*P*)	b. All mRNA targets for this miR (*P*)	6. miR function
miR-203a	541	Yes (1×10^{-5})	Down	$<1 \times 10^{-5}$	3×10^{-10}	Inhibits growth, self-renewal, migration, invasion, and EMT
miR-205-5p	545	Yes (3×10^{-26})	Down	$<1 \times 10^{-5}$	8×10^{-9}	Promotes apoptosis and inhibits growth, migration, invasion, and EMT
miR-452-5p	499	Yes (0.001)	Down	7×10^{-4}	2×10^{-8}	Reduces stem-like traits and tumorigenesis, EMT
miR-200b-3p[a]	562	Yes (1×10^{-14})	Down	0.03	1×10^{-15}	Reduces proliferation, migration, invasion, and EMT
miR-429[a]	562	Yes (5×10^{-13})	Down	0.005	1×10^{-15}	Inhibits proliferation and EMT
miR-141-3p[b]	557	Yes (1×10^{-5})	Down	0.02	6×10^{-10}	Inhibits EMT
miR-200a-3p[b]	554	Yes (8×10^{-5})	Down	0.009	1×10^{-9}	Inhibits EMT
miR-7-5p	544	Yes (3×10^{-14})	Down	0.04	4×10^{-9}	Inhibits invasion, self-renewal, and EMT and promotes apoptosis
miR-138-5p	546	Yes (0.04)	Down	0.01	0.003	Inhibits proliferation, invasion, and migration and modifies DNA damage response
miR-34a-5p	539	Yes (0.0001)	Down	2×10^{-4}	1×10^{-4}	Inhibits proliferation, invasion, metastasis, stemness, EMT
miR-142-3p	522	Yes (0.03)	Down	0.04	5×10^{-9}	Maintenance of dendritic cells and inhibits growth and stemness
miR-33b-5p	483	Yes (0.0005)	Down	0.03	2×10^{-5}	Reduces proliferation and induces G_1 arrest and cholesterol transport

NOTE: Properties of the miRs and their associated mRNA targets that were significantly correlated with radioresistance. Column 1, miR name. Column 2, the number of predicted mRNAs that are being targeted by this miR. Column 3, a significant negative correlation between the miR and its predicted targets indicates that this miR is actively degrading its targets. Column 4, the direction of the miR expression in the group of resistant cell lines. Column 5a, *P* values from the BRB array tools time course plug-in, representing the correlation between radioresistance (AUC) and the expression of the miR over the 2 measured time points. Column 5b, *P* value of a two-sided *t* test comparing the difference between all *P* values for the Pearson correlations between the predicted mRNA targets and radioresistance versus all *P* values for the correlations between the nontarget mRNAs and radioresistance. Column 6, all references for the described miR functions can be found in Supplementary Table S3.

[a]Both members of miR family miR-200bc/429/548a.

[b]Both members of miR family miR-141/200a.

addition, only genes were selected that showed a fold change in the same direction (up- or downregulation) in both cell line pairs, which resulted in a set of 1,189 genes (Supplementary Table S7).

For each cell line, a score was generated for each gene set, by either calculating the mean expression of the genes in the set or in the case of the HNSCC EMT signature by calculating the Pearson correlation between the expression of the cell line and the average expression in FaDu-HIF1α(ΔODD) and UT-SCC-43A-Snail cell lines for these 1,189 genes. Next, scores for the gene sets were compared with the radiosensitivity values. Of the different gene sets, the HNSCC EMT gene set was the best predictor of radiosensitivity (linear regression *P*: 0.001) in the panel of 32 HNSCC cell lines, with a Spearman correlation of 0.74 ($P < 0.0001$). A plot of the HNSCC EMT score against the radiosensitivity is shown in Fig. 4, the individual scores per cell line can be seen in Supplementary Table S6.

Of note is that the two EMT-inducible cell lines, although HNSCC cells, were not part of the 32 cell line panel and thus were an independent test system, strengthening the interpretation of an EMT-based mechanism for radioresistance.

miRs predicting radiotherapy response in patients. The expression of the most significant miR in cell lines (miR-203) was tested in a pilot series of 34 patients with T2-3 larynx tumors treated with radiotherapy. The 12 top miRs were analyzed. When two groups created were divided by the median expression, a trend was seen for higher recurrence percentages with low expression of miR-452 (HR, 0.5; $P = 0.1$), miR-200b (HR, 0.7; *P*, 0.4), and miR-141

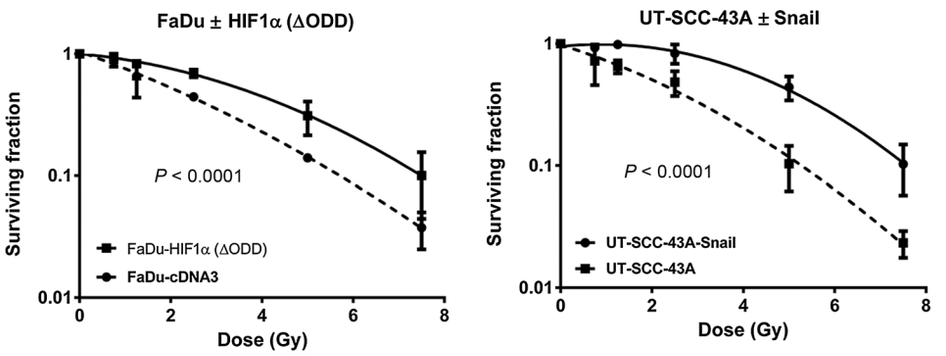

Figure 3.
Induction of EMT causes radioresistance. Induction of EMT by HIF1α (left) or Snail (right) leads to increased radioresistance.

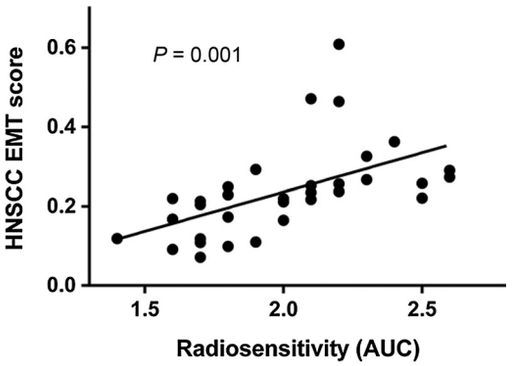

Figure 4.
HNSCC EMT score versus radiosensitivity. Cells with a higher score for EMT (more mesenchymal) are more resistant to irradiation.

(HR, 0.6; $P = 0.4$). However, only low miR-203 expression was significantly correlated with local recurrence in a multivariate Cox regression (Fig. 5; HR, 0.364; log-rank $P = 0.04$). These findings are in line with the cell line data, that is, loss of miR-203 expression leads to radioresistance.

Discussion

It is not clear why some cells are radiosensitive and others are intrinsically radioresistant. By identifying the underlying mechanisms of radioresistance, it should become possible to personalize therapy where necessary, thereby achieving better treatment success rates. In this study, we correlated expression of miRNA and mRNA to intrinsic radiosensitivity of head and neck cancer. In our HNSCC cell line panel, we found that a low expression of certain miRs was strongly correlated with radioresistance. Different analysis methods led to the conclusion that EMT was an important factor in radioresistance, namely, the top correlating mRNAs, miRs, and gene sets were all involved in EMT and these findings were validated by testing two different cell lines engineered to undergo EMT, which caused an increase in resistance. Next, we have shown that low expression of the top miR (miR-203) predicting intrinsic radiosensitivity indeed corresponded to more local recurrences after radiotherapy in a patient series of laryngeal carcinomas. Because it has previously been reported that no major difference was detected in miR profiles among laryngeal, oropharyngeal, or hypopharyngeal cancers, we believe that this cohort could be representable for all of these subsites (36). It should be noted that results were obtained using multiple testing on a small series, needing further validation in a larger cohort of head and neck squamous cell carcinomas, preferably including head and neck tumors from different subsites.

Although separate EMT genes like fibronectin 1, Snail, Slug, and E-cadherin have already been associated with radioresistance (37–40), it has not been clarified why EMT would cause radioresistance. We hypothesize that simultaneous with acquiring a mesenchymal phenotype, the mechanisms by which cells can become more resistant to irradiation are altered. EMT is mainly a description of a phenotype, but the fact that the acquisition of this phenotype is correlated with radioresistance may indicate it affects at least one of the three known mechanisms that lead to resistance: less damage upon irradiation, better repair of irradiation damage, or less cell death upon damage.

A first hypothesis could be that the evasion of DNA damage could lead to radioresistance (31). In a recent overview, Watson proposed that mesenchymal cancer cells possess heightened amounts of antioxidants that reduce damage caused by irradiation-induced reactive oxygen species (ROS; ref. 41). Gammon and colleagues showed that within mesenchymal cancer cells under normoxic conditions, a subpopulation of cells with low oxygen and ROS levels can be found (42).

Second, a more effective DNA damage repair system can lead to increased survival of cells after radiotherapy. This appears to be the case in breast cancer cell lines, in which it was shown that HOXB9 induces both EMT and confers resistance to ionizing radiation by accelerating the DNA damage response (43). In another report, it was shown that ATM-mediated Snail serine 100 phosphorylation regulates cellular radiosensitivity (44).

Finally, damaged cells can evade cell death and thereby survive irradiation. Kurrey and colleagues propose a model in ovarian cancer, in which EMT transcription factors Snail and Slug can antagonize p53-mediated apoptosis (40). TGFβ is also known to simultaneously invoke EMT and block apoptosis via PI3K signaling (45). In addition, another EMT inducer, SIP1, has been ascribed antiapoptotic properties (46). With the acquisition of an EMT phenotype, cells have been shown to increase autophagy: a lysosomal degradation pathway that can be used to increase survival of cells (47). Rouschop and colleagues demonstrated that inhibition of autophagy sensitized xenografts to irradiation (48).

In an attempt to confirm these hypotheses, we tested different gene sets for reactive oxygen species, DNA repair, cell-cycle phase, and several means of cell death against the EMT gene set (Supplementary Table S7). From these analyses, it appears that there is

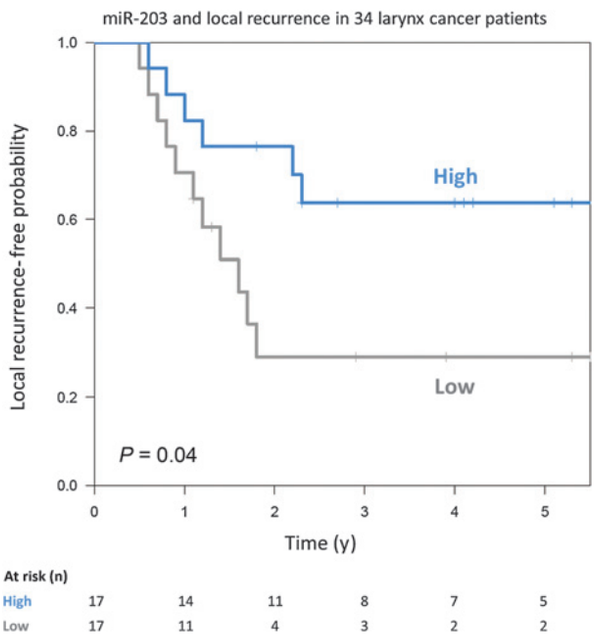

Figure 5.
miR-203 in patients. Seventeen patients with a local recurrence after radiotherapy were matched with 17 patients without a local recurrence. Patients with a high miR-203 expression had a significantly higher cure rate. The mean survival in this curve is 50% because of matching 1:1.

no single explanation for the radioresistance of the mesenchymal phenotype. The acquisition of a heightened EMT gene expression profile corresponds to a higher expression of genes known to be expressed in G_2, genes involved in DNA double-strand break repair and autophagy. This indicates that mesenchymal cells might become more resistant to radiotherapy by prolonging time spent in G_2, more efficient double-strand break repair, and the use of autophagy as a possible mechanism to evade cell death. ROS scavenger or apoptosis gene sets showed no correlation with expression of EMT genes.

Our study is the first to identify miRs with their mRNA targets that are involved in radioresistance in HNSCC. By analyzing miRs together with their targets, a more realistic representation of what occurs in cells can be obtained. A pitfall remains the allocation of the correct targets to every miR. Despite this possible confounding effect of wrongly allocated targets in the analysis, when studying the effect of all targets of one miR as a group, a reliable target effect can be observed. Future studies into correctly defining miR targets should improve this analysis method. The potential advantage of discovering miRs that are correlated with resistance is that, when used as therapeutic agents, they are able to target many genes at once, frequently within one pathway or network (49).

We observed that constitutive but not radiation-responsive genes correlated with radioresistance. These findings are consistent with findings of Birrell and colleagues on the yeast deletion mutant library (50) and the findings in the gene expression series of Amundson and colleagues who concluded that in the NCI-60 cell line panel "basal expression patterns discriminated well between radiosensitive and more resistant lines, possibly being more informative than radiation response signatures" (8).

In conclusion, the pre-irradiation miR-203 status, determined by integrative miR and mRNA analyses, was the most powerful predictor of radioresistance in our HNSCC cell line panel. This EMT-inhibiting miR was decreased in patients with a local recurrence after radiotherapy. The fact that radioresistance could be best predicted from baseline expression suggests that future studies into intrinsic resistance should not focus on response to irradiation. If these findings can be translated to the clinical setting, it should be possible to predict radiotherapy outcome from a pretreatment sample.

The next step would be to reverse EMT *in vivo*, possibly by restoring expression of miR-203. Because one miR can target many genes, EMT caused via different routes could potentially be inhibited by a single miR. Inhibition of EMT *in vivo* could not only make cells more radiosensitive but also more chemosensitive and less invasive, which together should lead to better patient survival.

Disclosure of Potential Conflicts of Interest

No potential conflicts of interest were disclosed.

Authors' Contributions

Conception and design: M.C. de Jong, A.C. Begg
Development of methodology: M.C. de Jong, A.C. Begg
Acquisition of data (provided animals, acquired and managed patients, provided facilities, etc.): M.C. de Jong, Grénman, R. Kerkhoven, M.W.M. van den Brekel, A.C. Begg
Analysis and interpretation of data (e.g., statistical analysis, biostatistics, computational analysis): M.C. de Jong, J.J. ten Hoeve, L.F. Wessels, M. Verheij, A.C. Begg
Writing, review, and/or revision of the manuscript: M.C. de Jong, H. te Riele, M.W.M. van den Brekel, M. Verheij, A.C. Begg
Administrative, technical, or material support (i.e., reporting or organizing data, constructing databases): M.C. de Jong, J.J. ten Hoeve, R. Grénman
Study supervision: M.W.M. van den Brekel, M. Verheij, A.C. Begg

Acknowledgments

The authors thank Wim Brugman, Janneke Kruizinga, and Marja Nieuwland for conducting the microarray experiments; Sander Canisius and Arno Velds for their advice on statistical modeling; and Iris de Rink for processing the raw miR sequencing data. They also acknowledge the NKI-AVL Core Facility Molecular Pathology and Biobanking (Dennis Peters, Annegien Broeks, and Linde Braaf) for supplying NKI-AVL Biobank material and laboratory support. They thank Manon Verwijs for her help with experiments.

Grant Support

This study was partly funded by the Dutch Cancer Society (NKI-2007-3941) and the Verwelius foundation.

The costs of publication of this article were defrayed in part by the payment of page charges. This article must therefore be hereby marked *advertisement* in accordance with 18 U.S.C. Section 1734 solely to indicate this fact.

Received February 24, 2015; revised July 23, 2015; accepted August 3, 2015; published OnlineFirst August 11, 2015.

References

1. Berrington de Gonzalez A, Curtis RE, Kry SF, Gilbert E, Lamart S, Berg CD, et al. Proportion of second cancers attributable to radiotherapy treatment in adults: a cohort study in the US SEER cancer registries. Lancet Oncol 2011;12:353–60.
2. Bourhis J, Overgaard J, Audry H, Ang KK, Saunders M, Bernier J, et al. Hyperfractionated or accelerated radiotherapy in head and neck cancer: a meta-analysis. Lancet 2006;368:843–54.
3. Knegjens J, Hauptmann M. Tumor volume as prognostic factor in chemoradiation for advanced head and neck cancer. Head Neck 2011;33:375–82.
4. Gasparini G, Bevilacqua P, Bonoldi E, Testolin A, Galassi A, Verderio P, et al. Predictive and prognostic markers in a series of patients with head and neck squamous cell invasive carcinoma treated with concurrent chemoradiation therapy. Clin cancer Res 1995;1:1375–83.
5. Rios Velazquez E, Hoebers F, Aerts HJWL, Rietbergen MM, Brakenhoff RH, Leemans RC, et al. Externally validated HPV-based prognostic nomogram for oropharyngeal carcinoma patients yields more accurate predictions than TNM staging. Radiother Oncol 2014;113:324–30.
6. Begg AC. Predicting recurrence after radiotherapy in head and neck cancer. Semin Radiat Oncol 2012;22:108–18.
7. Björk-Eriksson T, West C, Karlsson E, Mercke C. Tumor radiosensitivity (SF2) is a prognostic factor for local control in head and neck cancers. Int J Radiat Oncol Biol Phys 2000;46:13–9.
8. Amundson SA, Do KT, Vinikoor LC, Lee RA, Koch-Paiz Ca, Ahn J, et al. Integrating global gene expression and radiation survival parameters across the 60 cell lines of the National Cancer Institute Anticancer Drug Screen. Cancer Res 2008;68:415–24.
9. Torres-Roca JF, Eschrich S, Zhao H, Bloom G, Sung J, McCarthy S, et al. Prediction of radiation sensitivity using a gene expression classifier. Cancer Res 2005;65:7169–76.
10. Hall JS, Iype R, Senra J, Taylor J, Armenoult L, Oguejiofor K, et al. Investigation of radiosensitivity gene signatures in cancer cell lines. PLoS One 2014;9:e86329.
11. Lim LP, Lau NC, Garrett-engele P, Grimson A. Microarray analysis shows that some microRNAs downregulate large numbers of target mRNAs. Nature 2005;433:769–73.
12. Lewis BP, Burge CB, Bartel DP. Conserved seed pairing, often flanked by adenosines, indicates that thousands of human genes are microRNA targets. Cell 2005;120:15–20.

13. Bagga S, Bracht J, Hunter S, Massirer K, Holtz J, Eachus R, et al. Regulation by let-7 and lin-4 miRNAs results in target mRNA degradation. Cell 2005;122:553–63.
14. Friedman R, Farh K, Burge C, Bartel D. Most mammalian mRNAs are conserved targets of microRNAs. Genome Res 2009;19:92–105.
15. Morozova N, Zinovyev A, Nonne N, Pritchard L, Gorban AN, Harel-bellan A. Kinetic signatures of microRNA modes of action. RNA 2012;18: 1635–55.
16. Selbach M, Schwanhäusser B, Thierfelder N, Fang Z, Khanin R, Rajewsky N. Widespread changes in protein synthesis induced by microRNAs. Nature 2008;455:58–63.
17. Niemoeller OM, Niyazi M, Corradini S, Zehentmayr F, Li M, Lauber K, et al. MicroRNA expression profiles in human cancer cells after ionizing radiation. Radiat Oncol 2011;6:29.
18. Mueller AC, Sun D, Dutta A. The miR-99 family regulates the DNA damage response through its target SNF2H. Oncogene 2013;32:1164–72.
19. Liu Y-J, Lin Y-F, Chen Y-F, Luo E-C, Sher Y-P, Tsai M-H, et al. MicroRNA-449a Enhances Radiosensitivity in CL1-0 Lung Adenocarcinoma Cells. PLoS One 2013;8:e62383.
20. Lynam-Lennon N, Reynolds J V, Marignol L, Sheils OM, Pidgeon GP, Maher SG. MicroRNA-31 modulates tumour sensitivity to radiation in oesophageal adenocarcinoma. J Mol Med 2012;90:1449–58.
21. Takkunen M, Grenman R, Hukkanen M, Korhonen M, García de Herreros A, Virtanen I. Snail-dependent and -independent epithelial-mesenchymal transition in oral squamous carcinoma cells. J Histochem Cytochem 2006;54:1263–75.
22. Yang M-H, Wu M-Z, Chiou S-H, Chen P-M, Chang S-Y, Liu C-J, et al. Direct regulation of TWIST by HIF-1alpha promotes metastasis. Nat Cell Biol 2008;10:295–305.
23. Grenman R, Burk D, Virolainen E, Wagner JG, Lichter AS, Carey TE. Radiosensitivity of head and neck cancer cells in vitro. A 96-well plate clonogenic cell assay for squamous cell carcinoma. Arch Otolaryngol Neck Surg 1988;114:427–31.
24. Grénman R, Carey TE, McClatchey KD, Wagner JG, Pekkola-Heino K, Schwartz DR, et al. In vitro radiation resistance among cell lines established from patients with squamous cell carcinoma of the head and neck. Cancer 1991;67:2741–7.
25. Carlson M, Falcon S, Pages H, Li N. lumiHumanAll.db: me Human Illumina annotation data (chip lumiHumanAll). R package version 1.18.0
26. R-Core-Team. R: a language and environment for statistical computing. Vienna, Austria: R Foundation for Statistical Computing. 2012. ISBN 3-900051-07-0. Available from: http://www.R-project.org.
27. Gentleman RC, Carey VJ, Bates DM, Bolstad B, Dettling M, Dudoit S, et al. Bioconductor: open software development for computational biology and bioinformatics. Genome Biol 2004;5:R80.
28. Vergoulis T, Vlachos IS, Alexiou P, Georgakilas G, Maragkakis M, Reczko M, et al. TarBase 6.0: capturing the exponential growth of miRNA targets with experimental support. Nucleic Acids Res 2012;40:D222–9.
29. Grimson A, Farh KK-H, Johnston WK, Garrett-Engele P, Lim LP, Bartel DP. MicroRNA targeting specificity in mammals: determinants beyond seed pairing. Mol Cell 2007;27:91–105.
30. Kalluri R, Weinberg RAR. The basics of epithelial-mesenchymal transition. J Clin Invest 2009;119:1420–8.
31. Diehn M, Cho RW, Lobo NA, Kalisky T, Dorie MJ, Kulp AN, et al. Association of reactive oxygen species levels and radioresistance in cancer stem cells. Nature 2009;458:780–3.
32. Winter SC, Buffa FM, Silva P, Miller C, Valentine HR, Turley H, et al. Relation of a hypoxia metagene derived from head and neck cancer to prognosis of multiple cancers. Cancer Res 2007;67:3441–9.
33. Chi J-T, Wang Z, Nuyten DSA, Rodriguez EH, Schaner ME, Salim A, et al. Gene expression programs in response to hypoxia: cell type specificity and prognostic significance in human cancers. PLoS Med 2006;3:e47.
34. Starmans MHW, Krishnapuram B, Steck H, Horlings H, Nuyten DSA, van de Vijver MJ, et al. Robust prognostic value of a knowledge-based proliferation signature across large patient microarray studies spanning different cancer types. Br J Cancer 2008;99:1884–90.
35. Glinsky G, Berezovska O, Glinskii A. Microarray analysis identifies a death-from-cancer signature predicting therapy failure in patients with multiple types of cancer. J Clin Invest 2005;115:1503–21.
36. Hui ABY, Lenarduzzi M, Krushel T, Waldron L, Pintilie M, Shi W, et al. Comprehensive MicroRNA profiling for head and neck squamous cell carcinomas. Clin Cancer Res 2010;16:1129–39.
37. Jerhammar F, Ceder R, Garvin S, Grénman R, Grafström RC, Roberg K. Fibronectin 1 is a potential biomarker for radioresistance in head and neck squamous cell carcinoma. Cancer Biol Ther 2010;10:1244–51.
38. Holz C, Niehr F, Boyko M, Hristozova T, Distel L, Budach V, et al. Epithelial-mesenchymal-transition induced by EGFR activation interferes with cell migration and response to irradiation and cetuximab in head and neck cancer cells. Radiother Oncol 2011;101:158–64.
39. Theys J, Jutten B, Habets R, Paesmans K, Groot AJ, Lambin P, et al. E-Cadherin loss associated with EMT promotes radioresistance in human tumor cells. Radiother Oncol 2011;99:392–7.
40. Kurrey NK, Jalgaonkar SP, Joglekar A V, Ghanate AD, Chaskar PD, Doiphode RY, et al. Snail and slug mediate radioresistance and chemoresistance by antagonizing p53-Mediated apoptosis and acquiring a stem-like phenotype in ovarian cancer cells. Stem Cells 2009;27:2059–68.
41. Watson J. Oxidants, antioxidants and the current incurability of metastatic cancers. Open Biol 2013;3:120144.
42. Gammon L, Biddle A, Heywood HK, Johannessen AC, Mackenzie IC. Subsets of cancer stem cells differ intrinsically in their patterns of oxygen metabolism. PLoS One 2013;8:e62493.
43. Chiba N, Comaills V, Shiotani B, Takahashi F, Shimada T, Tajima K, et al. Homeobox B9 induces epithelial-to-mesenchymal transition-associated radioresistance by accelerating DNA damage responses. Proc Natl Acad Sci U S A 2012;109:2760–5.
44. Boohaker RJR, Cui X, Stackhouse M, Xu B. ATM-mediated Snail Serine 100 phosphorylation regulates cellular radiosensitivity. Radiother Oncol 2013; 108:403–8.
45. Singh A, Settleman J. EMT, cancer stem cells and drug resistance: an emerging axis of evil in the war on cancer. Oncogene 2010;29:4741–51.
46. Sayan AE, Griffiths TR, Pal R, Browne GJ, Ruddick A, Yagci T, et al. SIP1 protein protects cells from DNA damage-induced apoptosis and has independent prognostic value in bladder cancer. Proc Natl Acad Sci U S A 2009;106:14884–9.
47. Akalay I, Janji B, Hasmim M, Noman MZ, André F, De Cremoux P, et al. Epithelial-to-mesenchymal transition and autophagy induction in breast carcinoma promote escape from T-cell-mediated lysis. Cancer Res 2013; 73:2418–27.
48. Rouschop KMA, van den Beucken T, Dubois L, Niessen H, Bussink J, Savelkouls K, et al. The unfolded protein response protects human tumor cells during hypoxia through regulation of the autophagy genes MAP1LC3B and ATG5. J Clin Invest 2010;120:127–41.
49. Iorio M V, Croce CM. MicroRNA dysregulation in cancer: diagnostics, monitoring and therapeutics. A comprehensive review. EMBO Mol Med 2012;4:143–59.
50. Birrell GW, Brown JA, Wu HI, Giaever G, Chu AM, Davis RW, et al. Transcriptional response of *Saccharomyces cerevisiae* to DNA-damaging agents does not identify the genes that protect against these agents. Proc Natl Acad Sci U S A 2002;99:8778–83.